Optica Applicata, Vol. XLIII, No. 4, 2013
DOI: 10.5277/oa130401

Influence of palladium chemical structure on hydrogen sensing properties of carbonaceous–palladium thin films

ANNA KAMIŃSKA*, SŁAWOMIR KRAWCZYK, MIROSŁAW KOZŁOWSKI

Tele and Radio Research Institute, Ratuszowa 11, 03-450 Warsaw, Poland

*Corresponding author: anna.kaminska@itr.org.pl

In this work we investigate nanocomposite carbonaceous–palladium (C–Pd) films prepared by physical vapor deposition. Such films are promising materials for hydrogen sensor applications. This is related to the highly selective hydrogen absorption by palladium nanocrystallites. The C–Pd films obtained in various technological conditions differ in structure and electrical properties. These films were characterized by SEM, EDS and FTIR spectroscopy. FTIR spectroscopy was used to determine the amount of palladium acetate and fullerene, incompletely decomposed during the deposition process. FTIR spectra enabled us to explain the differences in C–Pd films resistance based on palladium chemical structure. The possibility of the application of C–Pd films as active layers in hydrogen sensors was also studied. The results showed that synthesized C–Pd films containing palladium nanograins could be used for hydrogen sensing.

Keywords: C–Pd thin films, hydrogen sensor, FTIR spectroscopy.

1. Introduction

The development and more widespread use of hydrogen gas as an energy carrier has led to the increasing demand for fast and reliable hydrogen sensors. Palladium-based hydrogen sensors have been thoroughly explored because of their highly selective interaction with hydrogen [1]. The interaction between hydrogen and palladium begins with H_2 adsorption on the palladium surface following the homolytic dissociation of H_2 molecules to H atoms. These hydrogen atoms diffuse into the Pd lattice and occupy its interstitial sites, forming solid solution [2]. At higher hydrogen pressure, further incorporation of hydrogen atoms induces phase transition from the α- to β-phase and formation of palladium hydride [3]. The Pd–H system is characterized by larger volume, different optical properties, lower work function and higher resistance compared to pure Pd [4]. Hydrogen sensing is based on changes in these properties. The palladium-based sensors include palladium thin films [5, 6], Pd nanowires [2, 7], Pd nanoparticle layers [8, 9] and C–Pd composites [10, 11].

The sensing mechanism of C–Pd films is based on Pd resistance changes in the presence of hydrogen which can be related to hydrogen concentration. Such sensors may be in the form of multi-walled carbon nanotubes (MWCNTs) decorated with palladium nanoparticles [10] or palladium nanoparticles embedded in a carbonaceous matrix. Systems based on MWCNTs can be prepared by the reduction of palladium in solution and the subsequent filtering of the aqueous suspension of decorated nanotubes [10]. Such sensors have low sensitivity (2.15% with 200 s response time at 0.21% H_2) and very slow recovery.

Therefore, C–Pd films containing palladium nanograins incorporated in a carbon matrix seem to be promising materials for hydrogen sensing applications. Such materials are investigated in this paper. In our work we studied the influence of the palladium chemical form on hydrogen sensing properties of C–Pd films obtained using the physical vapor deposition (PVD) method in H_2 sensors. We found that films only in which palladium acetate decomposed during preparation into metallic palladium could be used in hydrogen sensing. The sensitivity of our C–Pd films increases with H_2 concentration and exceeds 11% at 1% H_2.

2. Experiment

The nanocomposite C–Pd films were obtained using the PVD method [11]. In the PVD process, fullerene C_{60} (Sigma-Aldrich, 99.9%) and palladium acetate (Sigma-Aldrich, 99.98%) were used as film precursors. In the PVD process, various technological parameters were used to prepare samples with different structures and composition. Parameters of PVD process (intensity of current through sources (I_{C60} and I_{Pd}) and substrate temperature T) are shown in Tab. 1. The films were deposited on an alundum substrate. Conductive silver paint (SPI Supplies) was used to make electrical contacts to C–Pd films for resistance measurements.

T a b l e 1. Parameters of PVD process.

Sample	I_{C60} [A]	I_{Pd} [A]	T [°C]
S1	1.9	1.3	66
S2	2.1	1.2	45
S3	1.9	1.3	70
S4	1.9	1.2	69

The structure and morphology of obtained films were characterized by scanning electron microscopy (SEM). SEM investigations were carried out with a JEOL JSM-7600F field emission scanning electron microscope operating at 2 keV and 5 keV incident energy. The quantitative analysis of the composition of the C–Pd films was performed by energy dispersive spectroscopy (EDS). EDS measurements were performed with INCA ENERGY 250. The molecular structure of the C–Pd films was studied using Fourier transform infrared (FTIR) spectroscopy. FTIR measurements were performed with a ThermoScientific Nicolet iS10 FTIR spectrometer, using

the attenuated total reflectance (ATR) technique in a spectral range of 650–4000 cm^{-1} at a spectral resolution of 4 cm^{-1}.

Electrical measurements were performed using the indirect method on the basis of the voltage drop across a reference resistor connected in series with the investigated film. The films resistance was determined from the following formula:

$$R_{\mathrm{C-Pd}} = \frac{U_{\mathrm{sup}} - U_{\mathrm{ref}}}{U_{\mathrm{ref}} / R_{\mathrm{ref}}} \tag{1}$$

where $R_{\mathrm{C-Pd}}$ – C–Pd film resistance, U_{sup} – supply voltage, U_{ref} – the reference resistor voltage, R_{ref} – resistance of the reference resistor.

Hydrogen sensing measurements were performed in a special chamber, having an electrical feedthrough, gas flow inlet and outlet. Mass flow controllers were used to dilute hydrogen with N_2 to the chosen concentrations, with a total gas flow rate of 1 L/min. Measurements were carried out at room temperature and under atmospheric pressure. The electrical resistance of the C–Pd films was measured during their interaction with hydrogen. After stabilization of sample resistance, the flow of the H_2/N_2 mixture was cut off and air was introduced to the chamber to regenerate the films.

3. Results and discussion

3.1. SEM and EDS characterization

The topography and structure of the prepared C–Pd films was investigated by SEM (Fig. 1). SEM images show that the films are composed of grains with different shapes and diameters arranged layer by layer on the substrate. C–Pd films were deposited on the surface of ceramics, which has large surface area and roughness of the grains.

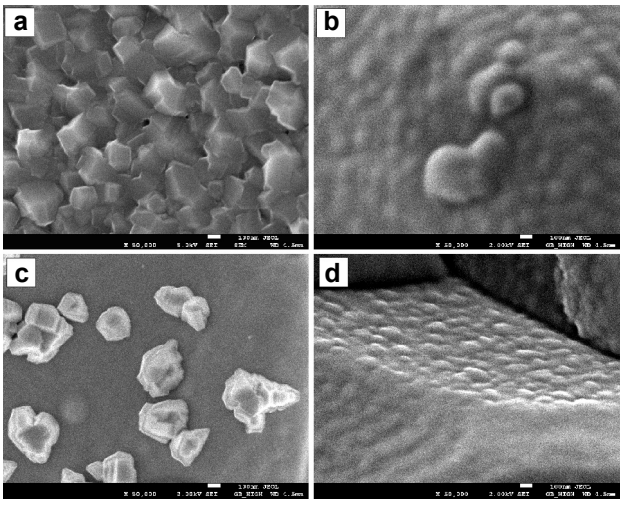

Fig. 1. SEM surface images of samples S1 (**a**), S2 (**b**), S3 (**c**) and S4 (**d**).

T a b l e 2. Palladium content and resistance of C–Pd films.

Sample	Pd [wt%]	R [kΩ]
S1	9.1	4.56
S2	9.3	unmeasurable*
S3	17.1	3.47
S4	17.4	unmeasurable*

* – R higher than 30 MΩ.

Depending on the PVD process parameters, the surface of C–Pd films has diverse morphology, shape and roughness of the grains. Figure 1 shows the differences in the roughness of the individual layers within a single grain of ceramics. On the surface of sample S1, densely packed tetrahedral carbonaceous grains with diameters between 100 and 250 nm are formed. Carbonaceous grains with gently rounded surfaces are visible. Bright objects visible on the surface of sample S3 are new C–Pd grains with a diameter larger than 200 nm being formed on a previously filled layer of the film.

The thickness of the studied films was measured by SEM method using sample fractures. All determined thicknesses of the films were about 300 nm. The content of palladium in the C–Pd films was determined by EDS. Due to the small thickness of the films, EDS analysis was performed using an accelerating voltage of 7 kV to minimize X-ray excitation volume. The results are shown in Table 2. It is clear that the Pd content in films S3 and S4 is similar and it is almost twice as high as in the other two samples.

3.2. FTIR spectroscopy

In Figure 2, FTIR spectra of palladium acetate and fullerene C_{60} (precursors of C–Pd films) are presented. In the spectrum of palladium acetate, three dominating absorption bands are found: a broadband in a wave number range of 1640 cm^{-1} and 1570 cm^{-1} associated with the asymmetric stretching vibrations of the C–O bond of the carboxylate groups, a band at 1430 cm^{-1} attributed to the symmetric stretching

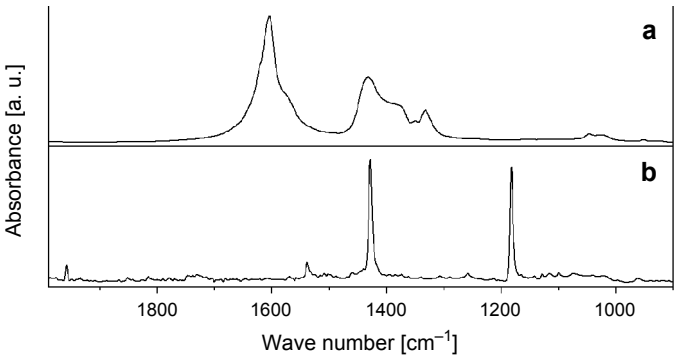

Fig. 2. FTIR spectra of palladium acetate (**a**) and fullerene (**b**).

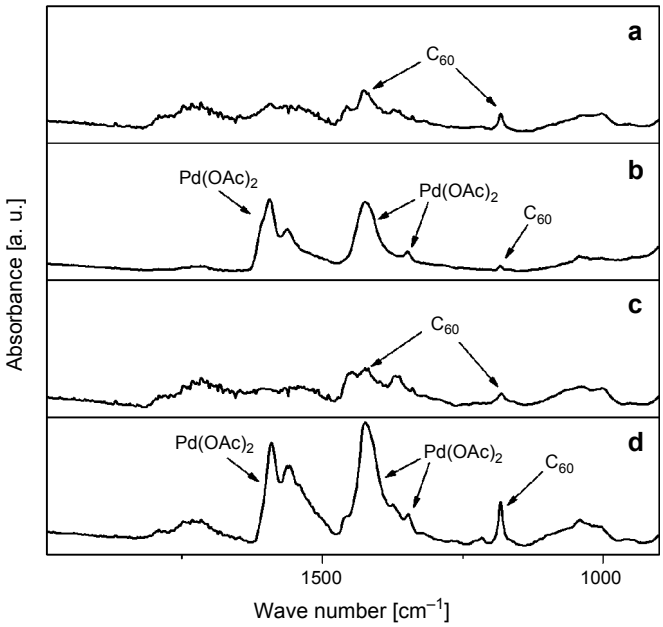

Fig. 3. FTIR spectra of films S1 (**a**), S2 (**b**), S3 (**c**) and S4 (**d**).

vibrations of the same C–O bond and a band at 1350 cm^{-1} from CH_3 bending vibrations [12]. The spectrum of fullerene exhibits two characteristics, very narrow bands at wave numbers of 1428 cm^{-1} and 1183 cm^{-1} assigned to C_{60} pentagon pinch and C_{60} pentagon asymmetric deformation, respectively [13].

In Figure 3, FTIR spectra of samples obtained in the PVD process are shown. In the spectra of samples S2 and S4, three bands corresponding to palladium acetate (1608–1540 cm^{-1}, 1422 cm^{-1} and 1349 cm^{-1}) are observed. The lack of bands originating from $Pd(OAc)_2$ in the spectra of films S1 and S3 indicates its complete decomposition to metallic palladium in the PVD process. The decomposition of palladium acetate is probably connected with the use of higher intensity of current through palladium source (see Table 1). The formation of *fcc* Pd nanocrystallites from palladium acetate during C–Pd film preparation was shown in our previous studies using the TEM method [14]. However, all samples contain fullerene C_{60}. In the spectra of samples S2 and S4, only one fullerene band (1183 cm^{-1}) is observed, because the second one (1428 cm^{-1}) overlaps with the band associated with the symmetric stretching vibrations of the C–O bond of $Pd(OAc)_2$ molecules. The highest intensity of the fullerene band in the spectrum of sample S4 means the largest C_{60} content in this film. All characteristic bands are indicated by arrows in Fig. 3.

3.3. Electrical measurements

The results of measurements of film electrical resistance are listed in Table 2. It is noted that two of the films (S1 and S3) have a resistance of about 3.5–4.5 kΩ, while

the other two samples have a non-conductive nature. The reason is the chemical structure of palladium in the investigated samples. No decomposition of palladium acetate to metallic Pd in the PVD process (see Fig. 3) results in the very high resistance of films S2 and S4, independently of the palladium content. This suggests that the nature of the carbon matrix is also non-conductive. The low resistance of films S1 and S3 is related to the presence of a metallic form of palladium. In the case of samples S1 and S3, an influence of the palladium content on film resistance was found. The increase in the amount of palladium in C–Pd films leads to their lower resistance.

3.4. Hydrogen sensing measurements

Hydrogen sensing characterization was performed for two samples: S1 and S3. The non-conductive character of samples S2 and S4 prevented sensing measurements. To investigate the reproducibility of sensing and to compare sample sensitivity and response time, the films were tested in four response-recovery cycles. The results for an atmosphere containing 1% H_2 are shown in Fig. 4 as a relationship between film sensitivity and time. Sensitivity ($\Delta R/R_0$) was calculated from the following equation:

$$\frac{\Delta R}{R_0} = \frac{R - R_0}{R_0} \times 100\% \tag{2}$$

where R is sample resistance in a test gas and R_0 is sample resistance in air. The introduction of hydrogen to the measurement chamber led to an increase in film resistance, while the introduction of air resulted in the resistance reaching its initial value again. The increased resistance in the presence of hydrogen is caused by the formation of Pd–H solid solution whose resistance is higher than that of metallic palladium [2, 4, 7]. The introduction of air leads to the decomposition of the Pd–H system resulting in lower film resistance. The sensing characteristics for both C–Pd films are fully repeatable. The sensitivity of film S1 is slightly higher, while the re-

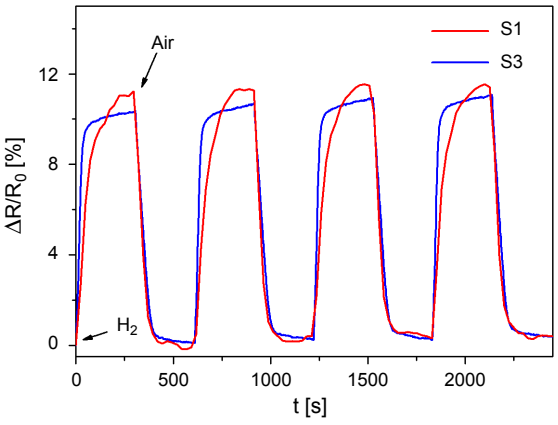

Fig. 4. C–Pd film sensitivity *vs*. time of exposure to 1% H_2.

sponse is 3.5 times slower than that of S3. The higher response rate of sample S3 is probably connected with higher palladium concentration. This can be explained by higher number of adsorption centers on the surface of palladium nanograins in the sample with higher Pd content. Higher number of active centers results in an increase of hydrogen adsorption rate and therefore leads to an increase of film response rate.

To investigate the influence of hydrogen concentration on the sensitivity and response time, sensing measurements for different [H_2] from 0.05% to 1% were carried out. The results are shown in Fig. 5. Response time $t_{90\%}$ is defined as time necessary to reach 90% of the maximum resistance change at a given hydrogen concentration. As can be seen in Fig. 5**a**, the sensitivity of both films increases with the hydrogen content in the atmosphere. Therefore, we can correlate the changes in sensor resistance with hydrogen concentration. The sensitivity of S1 is on average 10% higher than that of sample S3.

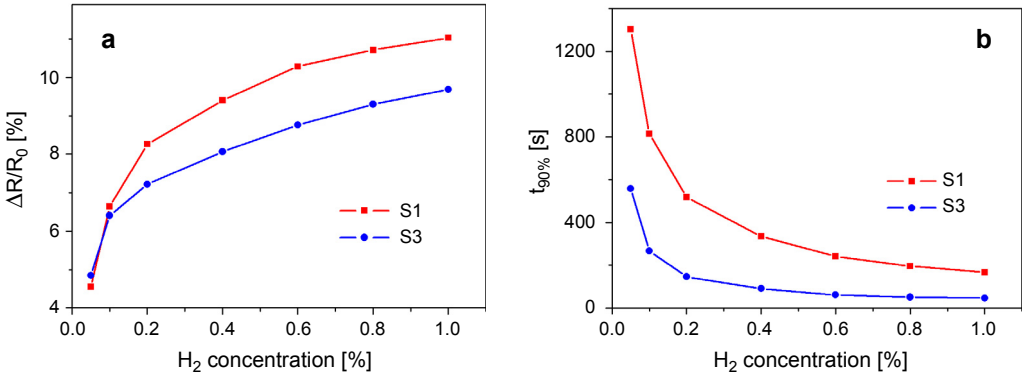

Fig. 5. C–Pd film sensitivity (**a**) and response time (**b**) *vs.* H_2 concentration.

With reference to Fig. 5**b**, it is noted that the response time becomes shorter with increasing H_2 concentration. The response time at 1% H_2 is 167 s and 46 s for films S1 and S3, respectively. The response of film S3 is about 3 times as fast as that of sample S3 throughout the range of tested hydrogen concentrations. The differences in the response rate can be explained by our EDS analysis. The faster response of film S3 results from the higher palladium content.

4. Conclusions

In this paper we investigated the hydrogen sensing properties of the C–Pd films obtained in the PVD process. The influence of the palladium chemical form on the application potential of these films in H_2 sensors was studied. The results showed that the decomposition of palladium acetate to metallic palladium was necessary for such an application. The sensitivity of the prepared C–Pd films increases with hydrogen concentration, allowing us to correlate sensor resistance changes with H_2 concentration in the surrounding atmosphere. The sensitivity of our C–Pd films exceeds 11%

and response time is less than 50 s at 1% H_2. It is concluded that the obtained films containing palladium nanograins placed in a carbonaceous matrix can be used as active layers in hydrogen sensors.

Acknowledgements – The authors thank Prof. E. Czerwosz and H. Wronka for the preparation of C–Pd films. This project is co-financed by the European Regional Development Fund within the Innovative Economy Operational Programme 2007–2013 No. UDA-POIG.01.03.01-14-071/08-08.

References

[1] JIN-SEO NOH, JUN MIN LEE, WOOYOUNG LEE, *Low-dimensional palladium nanostructures for fast and reliable hydrogen gas detection*, Sensors **11**(1), 2011, pp. 825–851.

[2] ZENG X.Q., LATIMER M.L., XIAO Z.L., PANUGANTI S., WELP U., KWOK W.K., XU T., *Hydrogen gas sensing with networks of ultrasmall palladium nanowires formed on filtration membranes*, Nano Letters **11**(1), 2011, pp. 262–268.

[3] FAN YANG, TAGGART D.K., PENNER R.M., *Joule heating a palladium nanowire sensor for accelerated response and recovery to hydrogen gas*, Small **6**(13), 2010, pp. 1422–1429.

[4] IBAÑEZ F.J., ZAMBORINI F.P., *Ozone- and thermally activated films of palladium monolayer-protected clusters for chemiresistive hydrogen sensing*, Langmuir **22**(23), 2006, pp. 9789–9796.

[5] EUNSONGYI LEE, JUN MIN LEE, JA HOON KOO, WOOYOUNG LEE, TAEYOON LEE, *Hysteresis behavior of electrical resistance in Pd thin films during the process of absorption and desorption of hydrogen gas*, International Journal of Hydrogen Energy **35**(13), 2010, pp. 6984–6991.

[6] XU T., ZACH M.P., XIAO Z.L., ROSENMANN D., WELP U., KWOK W.K., CRABTREE G.W., *Self-assembled monolayer-enhanced hydrogen sensing with ultrathin palladium films*, Applied Physics Letters **86**(20), 2005, article 203104.

[7] FAN YANG, SHENG-CHIN KUNG, MING CHENG, HEMMINGER J.C., PENNER R.M., *Smaller is faster and more sensitive: the effect of wire size on the detection of hydrogen by single palladium nanowires*, ACS Nano **4**(9), 2010, pp. 5233–5244.

[8] KHANUJA M., VARANDANI D., MEHTA B.R., *Pulse like hydrogen sensing response in Pd nanoparticle layers*, Applied Physics Letters **91**(25), 2007, article 253121.

[9] KHANUJA M., SHRESTHA S., MEHTA B.R., KALA S., KRUIS F.E., *Magnitude and time response of electronic and topographical changes during hydrogen sensing in size selected palladium nanoparticles*, Journal of Applied Physics **110**(1), 2011, article 014318.

[10] ZILLI D., BONELLI P.R., CUKIERMAN A.L., *Room temperature hydrogen gas sensor nanocomposite based on Pd-decorated multi-walled carbon nanotubes thin films*, Sensors and Actuators B: Chemical **157**(1), 2011, pp. 169–176.

[11] CZERWOSZ E., DŁUŻEWSKI P., KOZŁOWSKI M., SOBCZAK J.W., STARNAWSKA E., WRONKA H., *Electron emitting nanostructures of carbon + Pd system*, Molecular Crystals and Liquid Crystals **353**(1), 2000, pp. 237–242.

[12] FANG Q., HE G., CAI W.P., ZHANG J.-Y., BOYD I.W., *Palladium nanoparticles on silicon by photoreduction using 172 nm excimer UV lamps*, Applied Surface Science **226**(1–3), 2004, pp. 7–11.

[13] BYSZEWSKI P., KLUSEK Z., *Some properties of fullerenes and carbon nanotubes*, Opto-Electronics Review **9**(2), 2001, pp. 203–210.

[14] KOWALSKA E., CZERWOSZ E., KOZŁOWSKI M., SURGA W., RADOMSKA J., WRONKA H., *Structural, thermal, and electrical properties of carbonaceous films containing palladium nanocrystals*, Journal of Thermal Analysis and Calorimetry **101**(2), 2010, pp. 737–742.

Received April 18, 2013
in revised form July 25, 2013